Inorganic Chemistry

Article

pubs.acs.org/IC

Transmetalation of a Dodecahedral Na_9 Aggregate-Based Polymer: A Facile Route to Water Stable Cu(II) Coordination Networks

Jin-Xiang Chen,*[,†] Ming Chen,[†] Ni-Ni Ding,[‡] Wen-Hua Chen,[†] Wen-Hua Zhang,*[,‡,⊥] T. S. Andy Hor,*[,‡,§] and David J. Young*[,‡,∥]

[†]School of Pharmaceutical Sciences, Southern Medical University, ShaTai Road 1023, Guangzhou 510515, China

[‡]Institute of Materials Research and Engineering (IMRE), A*STAR, 3 Research Link, 117602 Singapore

[§]Department of Chemistry, National University of Singapore, 3 Science Drive 3, 117543 Singapore

[∥]School of Science, Monash University, 46150 Bandar Sunway, Selangor D.E., Malaysia

Supporting Information

ABSTRACT: A variety of network structures have been prepared by transmetalation of a polymer $\{Na_3[Na_9(Cbdcp)_6(H_2O)_{18}]\}_n$ (**1**) (Cbdcp = *N*-(4-carboxybenzyl)-(3,5-dicarboxyl)pyridinium) containing dodecahedral Na_9 aggregate secondary building units with Cu(II) by modulating the temperature, solvent, and pH. These complexes include a large, zwitterionic hexa-cuprometallocycle $[Cu_6(Cbdcp)_6(H_2O)_{18}]$ (**2**) formed in H_2O at room temperature, two three-dimensional polymers $[Cu_3(Cbdcp)_2(OH)_2(H_2O)_2]_n$ (**3**) and $\{[Cu_3(Cbdcp)_2(OH)_2]\cdot 2H_2O\}_n$ (**4**) isolated from H_2O and DMF/H_2O at 135 °C, and a mononuclear complex $[Cu(HCbdcp)_2(H_2O)_3]\cdot H_2O$ (**5**) from H_2O at 100 °C and pH = 6. All the complexes are robust and water stable. The crystal framework of macrocycle **2** is stable up to 100 °C under vacuum and selectively adsorbs CO_2.

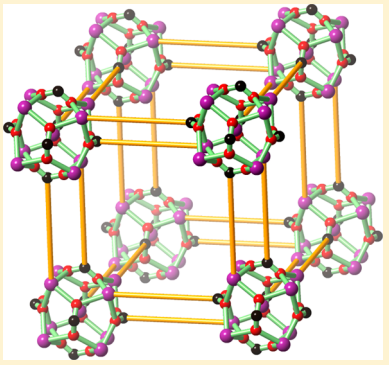

INTRODUCTION

Transmetalation is employed to prepare metal complexes that are otherwise difficult to make via direct metal−ligand assembly, and/or to increase conversion efficiencies of transformations yielding precious metal products.[1−8] The intermediate formation of Ag(I) carbene complexes as a high-yielding route to the corresponding Pd(II), Pt(II), and Au(I) carbenes is well-known.[9−13] Transmetalation involving metal−organic frameworks (MOFs) and other polymeric networks is challenging because of the low solubility of the polymer precursors. Literature examples are mostly isomorphous solid-state conversions[14] and can be considered as a subclass of postsynthetic modification—a useful method for introducing functionality into MOFs.[15−26] We herein report an unusual transmetalation route of a polynuclear sodium salt-aggregate $\{Na_3[Na_9(Cbdcp)_6(H_2O)_{18}]\}_n$ (**1**) (Cbdcp = *N*-(4-carboxybenzyl)-(3,5-dicarboxyl)-pyridinium) with Cu(II) as a convenient entry to an array of Cu(II) coordination complexes and networks in water. In contrast to the classic one-pot assembly of MOFs from metal ions and carboxylic acids in basic media at elevated temperatures, this method provides a soluble and isolable intermediate, facilitating fast and clean conversion even at ambient conditions with easy isolation of products. It also demonstrates a one-step deaggregation, and reassembly needed in a transmetalation process.

Complex **1** was prepared by neutralizing an aqueous suspension of tricarboxylic acid H_3CbdcpBr with dilute aqueous NaOH. Crystallization yielded a three-dimensional coordination polymer incorporating a dodecahedral $[Na_8(\mu_5\text{-}COO)_6(\mu_6\text{-}Na)]$ aggregate interconnected by tritopic $Cbdcp^{2-}$ ligands. The positively charged pyridinium group is balanced by deprotonation of one of the three carboxylic acids, leading to a pyridinium−carboxylate zwitterion (Chart 1). This ligand has a rotationally flexible CH_2 linkage that supports the diversity of network products with charged backbones, which plays an attractive role in MOFs to enhance interactions with gas molecules such as CO_2.[27−34]

Chart 1. Structures of H_3CbdcpBr and One of Its Zwitterionic Forms, H_2Cbdcp

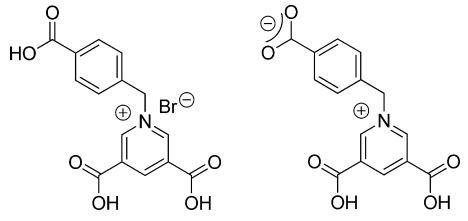

Transmetalation of $\{Na_3[Na_9(Cbdcp)_6(H_2O)_{18}]\}_n$ (**1**) with $Cu(NO_3)_2\cdot 3H_2O$ in the same stoichiometry under varied temperature, solvent, and pH yielded four Cu(II) complexes, including a zwitterionic Cu_6 metallocycle $[Cu_6(Cbdcp)_6$-

Received: April 3, 2014
Published: June 26, 2014

   dx.doi.org/10.1021/ic500789w | *Inorg. Chem.* 2014, 53, 7446−7454

Table 1. Crystallographic Data for Complexes 1−5

	1	2	3	4	5
molecular formula	$C_{15}H_{15}NNa_2O_9$	$C_{90}H_{90}Cu_6N_6O_{54}$	$C_{30}H_{24}Cu_3N_2O_{16}$	$C_{30}H_{24}Cu_3N_2O_{16}$	$C_{30}H_{28}CuN_2O_{16}$
fw	399.26	2500.92	859.13	859.13	736.08
cryst syst	trigonal	triclinic	monoclinic	monoclinic	orthorhombic
space group	$R\bar{3}$	$P\bar{1}$	$P2_1/c$	$P2_1/c$	$P2_12_12_1$
a (Å)	20.5520(12)	10.245(6)	26.3279(18)	6.2078(3)	8.3427(5)
b (Å)	20.5520(12)	18.977(11)	6.8162(5)	18.0634(8)	9.0471(5)
c (Å)	23.4904(13)	20.427(11)	8.1902(6)	13.7582(6)	38.228(2)
α (deg)	90.00	70.344(8)	90.00	90.00	90.00
β (deg)	90.00	82.436(9)	91.169(2)	101.1480(10)	90.00
γ (deg)	120.00	77.001(9)	90.00	90.00	90.00
V (Å^3)	8592.7(9)	3637(4)	1469.48(18)	1513.65(12)	2885.3(3)
Z	18	1	2	2	4
T/K	153(2)	296(2)	123(2)	100(2)	100(2)
D_{calc} (g cm^{-3})	1.389	1.142	1.942	1.885	1.694
λ (Mo Kα) (Å)	0.710 73	0.710 73	0.710 73	0.710 73	0.710 73
μ (cm^{-1})	0.152	0.936	3.312	2.175	0.846
total reflns	27 626	24 514	9805	22 743	36 029
unique reflns	3269	14 103	2391	3605	6853
no. observations	2917	8599	2193	3419	6553
no. params	268	577	214	241	473
R^a	0.0909	0.1150	0.0611	0.0257	0.0251
wR^b	0.2567	0.2679	0.1839	0.0740	0.0602
GOF^c	1.067	1.146	1.109	1.076	1.054
$\Delta\rho_{max}$ (e Å^{-3})	1.154	1.125	3.079	0.465	0.300
$\Delta\rho_{min}$ (e Å^{-3})	−1.100	−1.026	−1.453	−0.966	−0.359

^{a}R1 = $\Sigma||F_o| - |F_c||/\Sigma|F_o|$. ^{b}wR2 = $\{\Sigma[w(F_o^2 - F_c^2)^2]/\Sigma[w(F_o^2)^2]\}^{1/2}$. ^{c}GOF = $\{\Sigma[w(F_o^2 - F_c^2)^2]/(n-p)\}^{1/2}$, where n is the number of reflections and p is total number of parameters refined.

$(H_2O)_{18}]$ (**2**), two complexes with three-dimensional network structures $[Cu_3(Cbdcp)_2(OH)_2(H_2O)_2]_n$ (**3**) and $\{[Cu_3(Cbdcp)_2(OH)_2]\cdot 2H_2O\}_n$ (**4**), and a neutral mononuclear complex $[Cu(HCbdcp)_2(H_2O)_3]\cdot H_2O$ (**5**).

EXPERIMENTAL SECTION

All reagents and solvents were obtained from commercial sources and used without further purification. IR spectra were recorded on a Nicolet MagNa-IR 550 infrared spectrometer. Elemental analyses for C, H, and N were performed on an EA1112 CHNS elemental analyzer. Thermogravimetric analyses (TGA) were performed on a TA Instruments Q500 thermogravimetric analyzer at a heating rate of 10 °C/min under a nitrogen gas flow in an Al_2O_3 pan. Powder X-ray diffraction (PXRD) spectra were recorded with a Bruker D8 GADDS (general area detector diffraction system) microdiffractometer equipped with a VANTEC-2000 area detector with Φ rotation method. The X-ray generated from a sealed Cu tube was monochromated by a graphite crystal and collimated by a 0.5 mm MONOCAP (λ Cu Kα = 1.541 78 Å). The tube voltage and current were 40 kV and 40 mA, respectively. N_2 and CO_2 adsorption isotherms were carried out using a Micromeritics ASAP 2020 surface area and porosity analyzer. The samples were dried at 100 °C for 18 h before measurement. The dried sample tube equipped with a TranSeal (Micromeritics) was evacuated and weighed. The sample was transferred into the sample tube which was then capped by a TranSeal. The sample was heated to 100 °C under a vacuum of 2 mTorr for 2 h, at which point the outgas rate was less than 2 mTorr/min. The evacuated sample tube was weighed again, and the sample mass was determined by subtracting the mass of the previously weighed tube. The N_2 and CO_2 isotherms were measured using a liquid nitrogen bath (77 K) and dry ice/acetone (195 K), respectively.

Synthesis of H_3CbdcpBr. A DMF (20 mL) solution of 4-(bromomethyl)benzoic acid (4.30 g, 20 mmol) was added to 3,5-pyridinedicarboxylic acid (3.34 g, 20 mmol) in DMF (40 mL). After stirring 48 h at 60 °C, the resulting white precipitate was collected by filtration and washed with DMF (15 mL) and acetone (15 mL) to afford H_3CbdcpBr (6.11 g, 80%). Anal. Calcd. for $C_{15}H_{12}NO_6Br$: C 47.14, H 3.16, N 3.67. Found: C 46.98, H 3.55, N 3.55. IR (KBr disc, cm^{-1}) ν 3426 (m), 3073 (s), 1724 (s), 1644 (m), 1421 (m), 1315 (m), 1211 (s), 1170 (m), 1108 (s), 1021 (s), 764 (m), 748 (s), 695 (s), 637 (m), 589 (m), 537 (m), 449 (m).

Synthesis of $\{Na_3[Na_9(Cbdcp)_6(H_2O)_{18}]\}_n$ (1). H_3CbdcpBr (3.82 g, 10 mmol) was suspended in H_2O (50 mL) and the pH adjusted to 7.0 with 0.1 M NaOH solution. The clear, colorless solution was allowed to stand at room temperature for 3 weeks and provided colorless crystals of **1**, which were collected by filtration and dried *in vacuo*. Yield: 3.55 g (89%). ^{1}H NMR (400 MHz, D_2O) δ 9.21 (s, 2H), 9.08 (s, 1H), 7.84 (d, J = 10.4 Hz, 2H), 7.46 (d, J = 10.0 Hz, 2H), 5.88 (s, 2H). Anal. Calcd. for $C_{90}H_{90}N_6Na_{12}O_{54}\cdot 18H_2O$: C 39.74, H 4.67, N 3.09. Found: C 39.84, H 4.67, N 3.05. IR (KBr disc, cm^{-1}) ν 3410 (s), 1662 (s), 1625 (s), 1608 (s), 1546 (s), 1390 (s), 1357 (s), 1226 (m), 1167 (w), 1103 (w), 1020 (w), 912 (w), 852 (w), 817 (w), 770 (m), 726 (m), 707 (s), 642 (m), 507 (m), 462 (m).

Synthesis of Complexes 2−5. For step 1, a solution of complex **1** (119 mg, 0.05 mmol) in H_2O (40 mL) was added to $Cu(NO_3)_2\cdot 3H_2O$ (72.3 mg, 0.3 mmol) in H_2O (40 mL). The resulting mixture was stirred for 0.5 h to provide a clear light green solution.

*$[Cu_6(Cbdcp)_6(H_2O)_{18}]$ (**2**).* The green solution from step 1 was allowed to stand at room temperature for 2 weeks and provided needle-like crystals of **2**, which were collected by filtration, washed with H_2O, and dried *in vacuo*. Yield: 115 mg (92%). Anal. Calcd. for $C_{90}H_{90}Cu_6N_6O_{54}$: C 43.22, H 3.63, N 3.36. Found: C 42.95, H 3.52, N 3.33. IR (KBr disc, cm^{-1}) ν 3414 (s), 3068 (m), 2928 (w), 1653 (s), 1607 (s), 1559 (w), 1483 (w), 1368 (s), 1285 (w), 1207 (m), 1185 (m), 1166 (m), 1107 (s), 1020 (w), 991 (w), 925 (w), 873 (w), 852 (w), 793 (w), 766 (m), 727 (m), 650 (w), 620 (s), 473 (w).

*$[Cu_3(Cbdcp)_2(OH)_2(H_2O)_2]_n$ (**3**).* The green solution from step 1 was placed in a Teflon reactor and sealed in an autoclave before transferring to a programmable oven. The temperature of the oven was increased steadily from 25 to 135 °C over 4 h, kept at 135 °C for 72 h, and then cooled to room temperature over 48 h. The resulting blue prism crystals were filtered, washed with water, and dried *in vacuo* to provide **3**. Yield:

dx.doi.org/10.1021/ic500789w | Inorg. Chem. 2014, 53, 7446−7454

Scheme 1. Transmetalation Pathway of Complex 1 Aggregate-Salt to Cu(II) Complexes 2−5

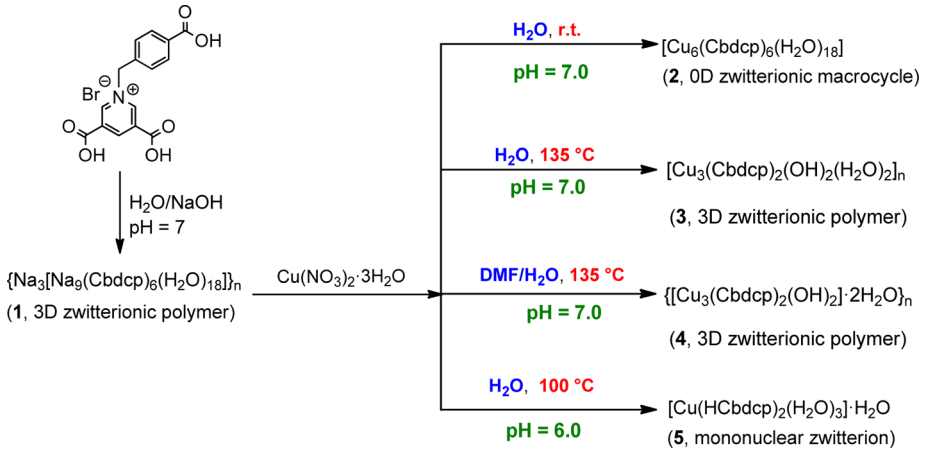

76 mg (89%). Anal. Calcd. for $C_{30}H_{24}Cu_3N_2O_{16}$: C 41.94, H 2.82, N 3.26. Found: C 42.03, H 2.92, N 3.13. IR (KBr disc, cm^{-1}) ν 3622 (m), 3314 (m), 3051 (m), 2988 (s), 1647 (s), 1605 (s), 1589 (s), 1542 (s), 1410 (s), 1396 (s), 1356 (s), 1221 (m), 1159 (m), 1027 (s), 1014 (s), 923 (w), 877 (m), 792 (m), 769 (s), 734 (s), 712 (s), 604 (m), 473 (m), 421 (m).

{[Cu$_3$(Cbdcp)$_2$(OH)$_2$]·2H$_2$O}$_n$ (4). DMF (5 mL) was added to the solution from step 1 in a Teflon reactor and heated using the same temperature profile as described for the preparation of **3**. The resulting green block crystals were washed with water and dried *in vacuo* to give **4**. Yield: 39 mg (45%). Anal. Calcd. for $C_{30}H_{24}Cu_3N_2O_{16}$: C 41.94, H 2.82, N 3.26. Found: C 42.33, H 2.57, N 3.22. IR (KBr disc, cm^{-1}) ν 3636 (m), 3315 (m), 3045 (m), 1649 (s), 1614 (s), 1600 (s), 1561 (s), 1371 (s), 1234 (m), 1170 (m), 1085 (s), 1019 (w), 957 (w), 930 (w), 842 (m), 798 (m), 768 (s), 734 (s), 721 (m), 652 (m), 577 (m), 495 (m), 470 (m).

[Cu(HCbdcp)$_2$(H$_2$O)$_3$]·H$_2$O (5). The pH of the green solution from step 1 was adjusted to 6.0 with 0.1 M HCl. This solution was then placed in a glass bottle and heated steadily in a programmable oven from 25 to 100 °C over 4 h. After 72 h at 100 °C, the oven was cooled to room temperature over 48 h. The resulting green, needle-like crystals were filtered, washed with water, and dried *in vacuo* to give **5**. Yield: 170 mg (77%). Anal. Calcd. for $C_{30}H_{28}CuN_2O_{16}$: C 48.95, H 3.83, N 3.81. Found: C 48.27, H 3.43, N 3.67. IR (KBr disc, cm^{-1}) ν 3057 (m), 2621 (m), 2506 (m), 1702 (s), 1642 (s), 1587 (s), 1398 (s), 1361 (s), 1270 (s), 1232 (m), 1171 (m), 1118 (m), 1028 (w), 1020 (w), 952 (w), 920 (w), 875 (m), 846 (m), 767 (s), 752 (m), 731 (m), 708 (m), 604 (w), 539 (w), 518 (m), 469 (m).

X-ray Crystallography for 1−5. Crystallographic measurements were made on a Bruker APEX II diffractometer by using graphite-monochromated Mo Kα (λ = 0.710 73 Å) irradiation for **1**−**5**. The data were corrected for Lorentz and polarization effects with the SMART suite of programs and for absorption effects with SADABS.[35] All crystal structures were solved by direct methods and refined on F^2 by full-matrix least-squares techniques with SHELXTL-97 program.[36] For **1**, the peak with the highest electron density was tentatively assigned as Na atom with its occupancy factor fixed at 0.5 to maintain charge neutrality of the molecule. This Na atom is therefore not participating in the structural discussion in the following section. For **5**, the structure was solved and refined in the orthorhombic space group $P2_12_12_1$. Platon suggested the higher symmetry *Pnma* space group, but refinement using a disordered model in *Pnma* gave an unsatisfactory *R* index of 0.18. The structure was thus refined in space group $P2_12_12_1$ with racemic twin domains to give final *R* indices of *R* = 0.0251; *wR* = 0.0609 with Flack parameter of 0.572(7). For **1**, **3**, **4**, and **5**, the hydrogen atoms on all of the H_2O molecules and OH^- groups were located from the difference Fourier map with their coordinates refined either freely (for **5**) or by applying distance restraints of O−H = 0.85 Å (for **1** and **3**) or O−H = 0.83 Å (for **4**) with all their thermal parameters constrained to $U_{iso}(H) = 1.2U_{eq}(O)$. For complex **2**, the location of the hydrogen atoms on water was suggested by the Calc-OH program in the WinGX suite,[37] and the water molecules were then refined as a rigid group with their thermal parameters constrained to $U_{iso}(H) = 1.2U_{eq}(O)$.

The solvent accessible voids occupy volumes of 769.4 Å^3 (9.0% of the total cell volume) for **1**, 1359.6 Å^3 (37.4% of the total cell volume) for **2**. These void spaces are filled with unidentifiable electron densities (tentatively assumed to be H_2O based on the FT-IR spectra), and their contributions to the scattering factors were removed by SQUEEZE.[38] Crystallographic data have been deposited with the Cambridge Crystallographic Data Center as supplementary publication numbers CCDC 990239−990243. These data can be either obtained free of charge from the Cambridge Crystallographic Data Centre via www.ccdc.cam.ac.uk/data_request/cif or from the Supporting Information. A summary of the key crystallographic data for **1**−**5** is listed in Table 1.

RESULTS AND DISCUSSION

Synthesis and Characterization of 1−5. A summary of the reaction conditions for each complex is depicted in Scheme 1. The precursor complex $\{Na_3[Na_9(Cbdcp)_6(H_2O)_{18}]\}_n$ (**1**) was obtained from the evaporation of an aqueous mixture of H_3CbdcpBr and NaOH. Further transmetalation reaction of **1** with $Cu(NO_3)_2{\cdot}3H_2O$ at room temperature provided a zwitterionic Cu_6 macrocycle $[Cu_6(Cbdcp)_6(H_2O)_{18}]$ (**2**). Complexes $[Cu_3(Cbdcp)_2(OH)_2(H_2O)_2]_n$ (**3**), $\{[Cu_3(Cbdcp)_2(OH)_2]{\cdot}2H_2O\}_n$ (**4**), and $[Cu(HCbdcp)_2(H_2O)_3]{\cdot}H_2O$ (**5**) could either be prepared from the reaction of **1** with $Cu(NO_3)_2{\cdot}3H_2O$ under the reaction conditions indicated or alternatively from **2** under identical conditions. The transmetalation is assumed to undergo a "disruptive exchange" mechanism.[14,39,40] In this mechanism, the individual sodium ions migrate from the Na_9 aggregate which triggers simultaneous copper−ligand reassembly to provide copper−carboxylate complexes.

Complexes **1**−**5** can be obtained in good yields and are air and moisture stable. Thermogravimetric analyses (TGA) indicated that **1** is stable up to 280 °C, whereas **2**−**5** are stable up to *ca.* 220 °C (Supporting Information Figures S1−S3). Their bulk phase purity was confirmed by FT-IR, elemental analysis, and powder X-ray diffraction (PXRD, Supporting Information Figures S4−S7).

Crystal Structure of {Na$_3$[Na$_9$(Cbdcp)$_6$(H$_2$O)$_{18}$]}$_n$ (1). Complex **1** reveals a three-dimensional structure with Na_9 aggregate as secondary building unit. Figure 1a illustrates its asymmetric unit in which one carboxylate bridges three Na atoms with separations of 4.17, 3.64, and 3.66 Å for Na1···Na2, Na2···Na3, and Na1···Na3, respectively. This triumvirate of sodium atoms

dx.doi.org/10.1021/ic500789w | Inorg. Chem. 2014, 53, 7446−7454

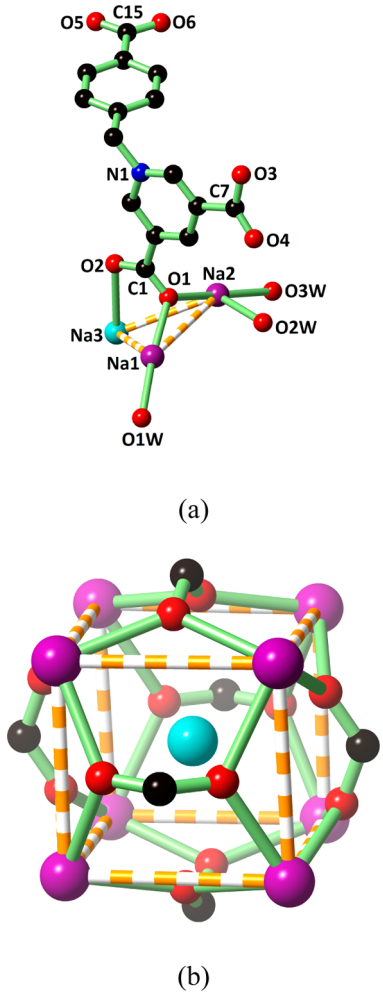

Figure 1. Structures of complex **1** showing (a) the asymmetric unit with labeling scheme, (b) the dodecahedral aggregate formed by Na1, Na2, and the face-capping μ_4-carboxylates (weak Na3···O interactions are omitted for clarity).

forms a Na_9 aggregate of secondary building unit in **1** which contains two Na1, six Na2, and one Na3 atoms. Na1 and Na2 form a cube, in which two Na1 atoms occupy the diagonal vertices of the cube and lie on the 3-fold rotational axis; six Na2 atoms occupy the remaining vertices and are separated in two parallel planes with a staggered conformation (Supporting Information Figure S8). Na3 is at the center of the cube on a 6-fold improper rotational axis. Each face of the cube is capped by one μ_4-carboxylate with each O atom associated with two Na atoms. A dodecahedron is formed by Na1, Na2, and the six face-capping μ_4-carboxylates and has Na3 located at the center and stabilized by 12 weak Na3···O interactions (2.770(3) Å, Figure 1b).

Each face of one cube is linked to an adjacent cube through a pair of $Cbdcp^{2-}$ ligands via the pyridinium dicarboxylate moiety (Figure 2a). The carboxylate involving C1, O1, and O2 caps the face of one cube while the carboxylate involving C7, O3, and O4 links to the adjacent aggregate in a monodentate fashion through a Na2−O3 bond (Figure 2a). Each dodecahedral Na_9 aggregate is therefore connected to six dodecahedral aggregates in three orthogonal directions (Figure 2b) through six pairs of $Cbdcp^{2-}$ ligands to form an enlarged cube (Figure 2c) and subsequently an extended network with *pcu* topology (Supporting Information Figure S9) as observed for MOF-5.[41−43] Notably, while MOF-5

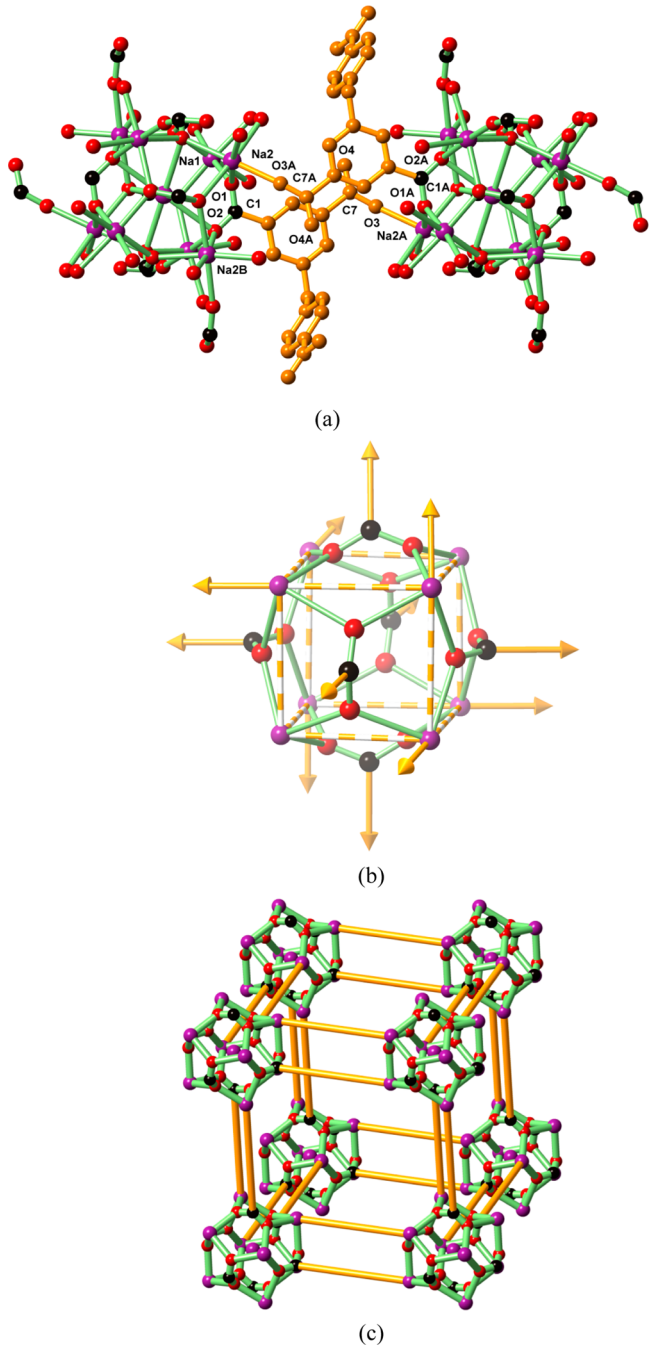

Figure 2. Structure of complex **1** showing (a) the two adjacent Na_9 aggregates bridged by a pair of $Cbdcp^{2-}$ ligands (highlighted in orange), (b) the aggregate with arrows indicating the general direction of connection to adjacent aggregates, (c) an enlarged cube formed by interconnection of eight Na_9 aggregates. Symmetry codes for part a: A $-x-3, -y, -z-1$; B $y-{}^{4}/_{3}, -x+y-{}^{5}/_{3}, -z-{}^{2}/_{3}$.

and its isoreticular networks contain Zn_4 aggregate bridged by a single organic bridge, complex **1** is uncommon in that (i) the aggregate is dodecahedral with nine metal atoms and (ii) the aggregates are linked through double organic bridges. The voids of the network are occupied by the uncoordinated benzylcarboxylates and solvated water molecules.

*Crystal structure of $[Cu_6(Cbdcp)_6(H_2O)_{18}]$ (**2**).* Complex **2** features a large zwitterionic hexa-cuprometallocycle (Figure 3a). This cycle contains six Cu(II) and six $Cbdcp^{2-}$ ligands and has a near rectangular shape with dimensions of approximately 28 × 15

dx.doi.org/10.1021/ic500789w | *Inorg. Chem.* 2014, 53, 7446−7454

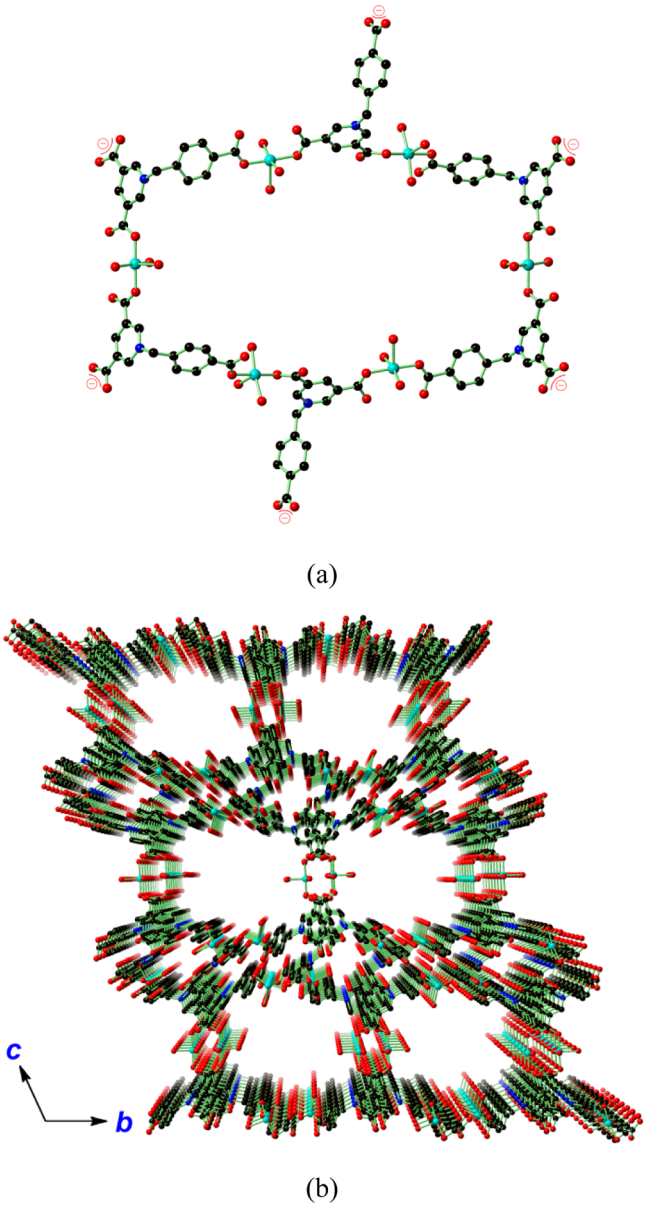

Figure 3. Structure of complex **2** showing (a) a big zwitterionic hexa-cuprometallocycle, and (b) the stacking of these zwitterionic cuprometallocycles along the *a* axis. Color codes: Cu (cyan), O (red), N (blue), C (black).

Å^2. The four pyridinium dicarboxylates form the corners of the rectangle, and monodentate coordination by one carboxylate to a single Cu(II) ion forms the shorter edge of the rectangle. The long edge is made up by two pendant benzylcarboxylates coordinating to two Cu(II) ions which, in turn, are bridged by a pyridinium dicarboxylate moiety. The six free uncoordinated carboxylates each carry a negative charge, thus maintaining overall charge neutrality of the hexa-cuprometallocycle. Each Cu atom displays a square pyramidal geometry with a pair of carboxylates bound in a monodentate coordination fashion and two water molecules in the equatorial plane, while the third water molecule occupies the apical position of the square pyramid. The C−O distances of the uncoordinated carboxylates fall in a narrow range 1.214(10)−1.257(12) Å, corroborating the charge delocalization on these carboxylates and the zwitterionic nature of the metallocycle.

The discrete cuprometallocycles form close contact with adjacent cycles by pairs of complementary hydrogen bonding (Supporting Information Table S6). One-dimensional channels (approximately 12 × 13 Å^2) are evident when looking along the crystallographic *a* axis, and these channels are filled with dissociated water molecules. PLATON[38] void space estimation revealed 1359.6 Å^3 per cell (37.4% of the total cell volume). The channels appended with uncoordinated carboxylates may further be used to bind other metal sources of interest to introduce new properties into the frameworks. The free-standing carboxylate groups may also function as catalyst for size selective organic transformations.[46]

Crystal Structure of $[Cu_3(Cbdcp)_2(OH)_2(H_2O)_2]_n$ (**3**). Complex **3** is a three-dimensional structure formed by carboxylate bridged 2D grids orthogonally linked by parallel, carboxylate and OH bridged one-dimensional chains. Each Cu1 has square planar coordination from a pair of *trans* μ-OH groups and a pair of *trans* μ-COO groups (Figure 4a). The μ-OH and μ-COO in turn bridge adjacent Cu1 atoms to propagate a chain along the *b* axis (Figure 4b). Each Cu2 atom has octahedral geometry with four μ-COO oxygen species in the equatorial plane and two aqua solvates in the axial positions (Figure 4a). Each Cu2 extends to four equivalent Cu2 atoms, forming a (4, 4) network extended in the *bc* plane (Figure 4c). The one-dimensional chains of Cu1 in the *b* direction (Figure 4b) and 2D grid in the *bc* plane (Figure 4c) are interconnected by $Cbdcp^{2-}$ ligands along the *a* axis to form a three-dimensional network (Figure 4d). The tilted $Cbdcp^{2-}$ ligand with a dihedral angle between the pyridinium ring and phenyl ring of 92.4° play an essential role in dictating the structure of **3**.

Crystal Structure of $\{[Cu_3(Cbdcp)_2(OH)_2]\cdot 2H_2O\}_n$ (**4**). Complex **4** is a three-dimensional polymer supported by one-dimensional rod-shaped polymeric chains running along the crystallographic *a* direction. These one-dimensional rods consist of an alternating arrangement of one six-coordinate Cu1 followed by a pair of five-coordinated Cu2 atoms (Figure 5a). The relative disposition of Cu atoms in this one-dimensional rod is similar to that reported for a discrete Cu4 aggregate by Zaworotko et al.[47] Within the one-dimensional rod, each Cu1 atom is coordinated by a pair of *trans* μ_3-OH and four μ-carboxylates. The μ_3-OH and μ-carboxylates in turn extend to four proximate Cu2 atoms propagating the chain. Each Cu2 is coordinated to a pair of μ_3-OH ligands, a pair of μ-carboxylates, and one additional monodentate carboxylate to furnish a square pyramidal geometry. The presence of μ_3-OH units in this structure is critical. They serve to balance one positive charge on Cu^{2+}, to bring together one Cu1 and two Cu2 atoms, and to stabilize the structure by forming a hydrogen bonding to the monodentate pyridyl carboxylate (Figure 5a). The ligands attached to the one-dimensional rod extend to six directions in the *bc* plane (Supporting Information Figure S10). The projecting carboxyl groups coordinate to six identical, neighboring rods and form a densely packed three-dimensional structure with small channels wherein two aqua solvates are encapsulated (Figure 5b).

Crystal Structure of $[Cu(HCbdcp)_2(H_2O)_3]\cdot H_2O$ (**5**). Complex **5** has a simple, mononuclear coordination structure consisting of a square pyramidal Cu(II), coordinated to three water molecules (one apical and two *cis* equatorial) and two, *cis* monodentate, pyridinium carboxylate bound $HCbdcp^-$ ligands (Figure 6). The free benzyl-COO groups are protonated, and the remaining pyridyl carboxylates balance the positive charge of the pyridinum cation and Cu(II) center.

dx.doi.org/10.1021/ic500789w | *Inorg. Chem.* 2014, 53, 7446−7454

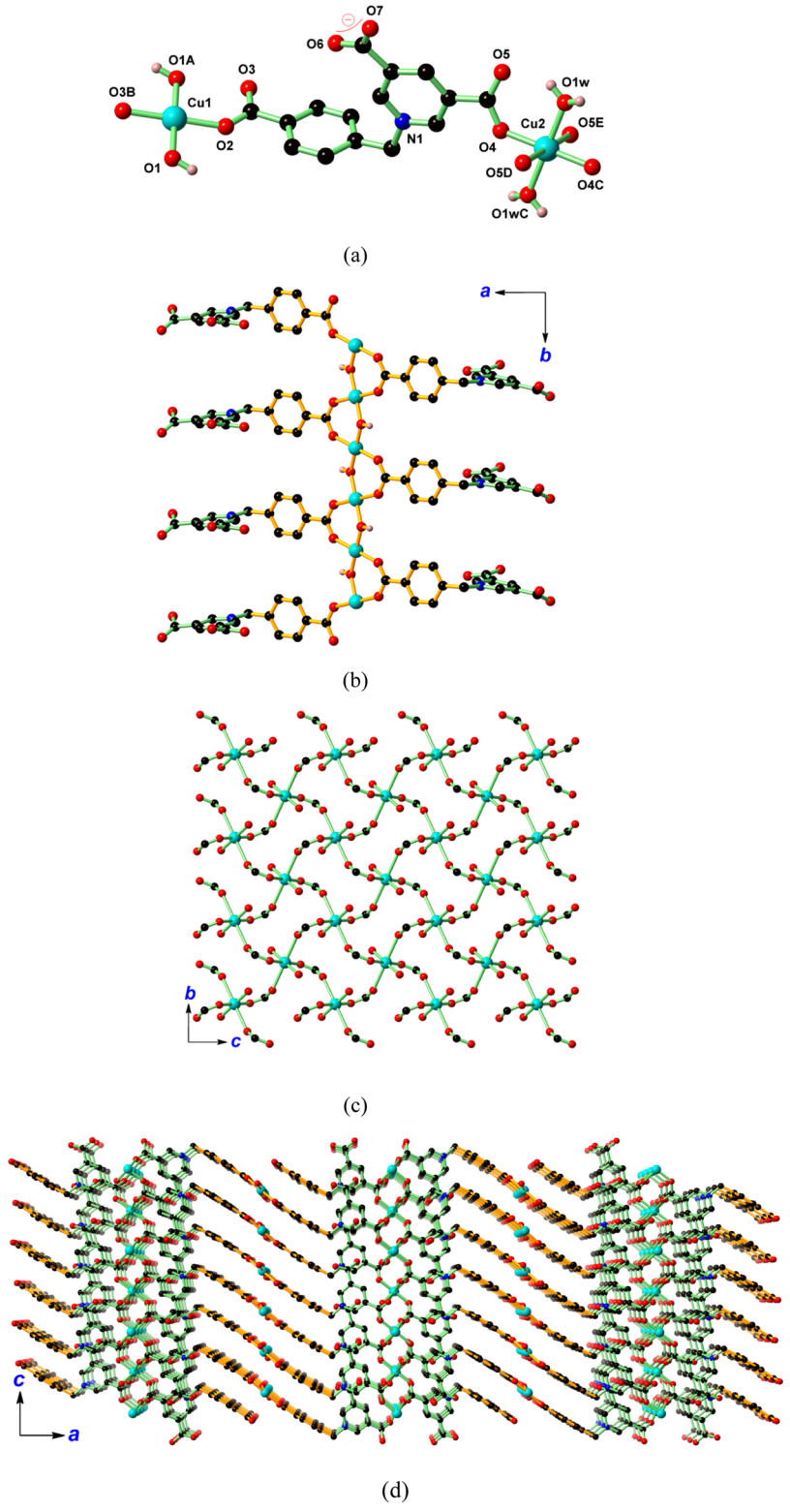

Figure 4. Structure of complex **3** showing (a) the asymmetric unit with the complete coordination environment around the Cu1 and Cu2 centers, (b) one-dimensional chain of Cu1 units propagated along the *b* direction, (c) 2D grid plane extended within the *bc* plane with only the Cu2 ions and bridging carboxylates shown for clarity, and (d) the three-dimensional structure looking along the *b* axis. Color codes: Cu (cyan), O (red), N (blue), C (black). Symmetry codes for part a: A $-x, y - 0.5, -z - 1.5$; B $-x, y + 0.5, -z - 1.5$; C $-x - 1, -y, -z$; D $-x - 1, y + 0.5, -z - 0.5$; E $x, -y - 0.5, z + 0.5$.

Stability and Porosity of 2. Thermogravimetric analysis (TGA) indicated that **2** is stable up to 220 °C. The first stage has a weight loss of 25.42% in the region 25−150 °C which corresponds to the loss of 41 H_2O molecules (theoretical value of 25.32%, including 23 dissociated and 18 coordinated H_2O molecules). After applying vacuum for 18, 36, and 72 h at 100 °C, the losses of 31, 32, and 34 H_2O molecules were found for complex **2** (Supporting Information Figure S2). Powder X-ray diffraction (PXRD) further indicated that the structure was maintained when vacuum was applied to the sample from 18 to

dx.doi.org/10.1021/ic500789w | *Inorg. Chem.* 2014, 53, 7446−7454

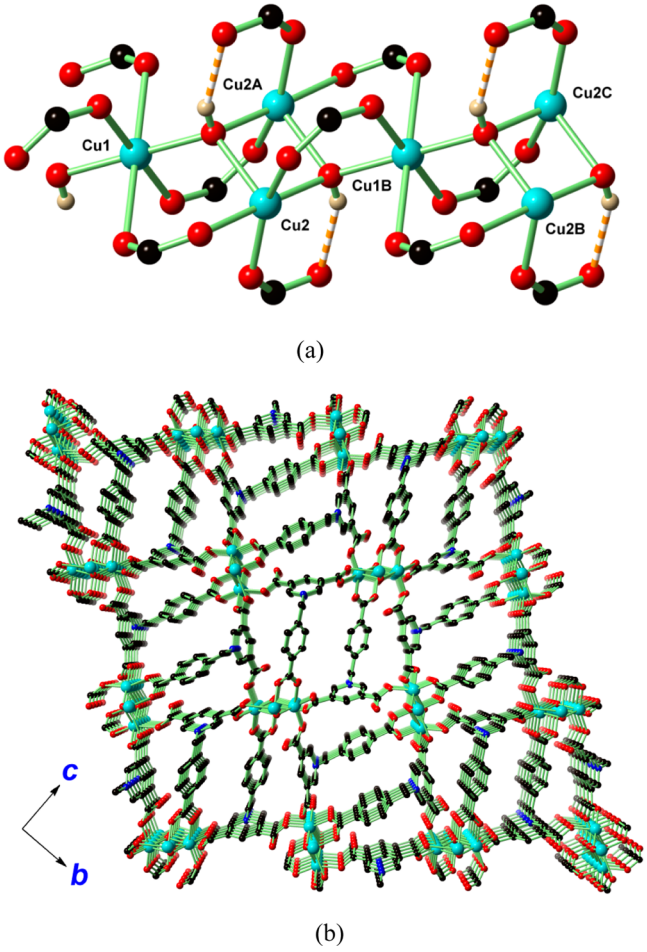

Figure 5. Structure of complex **4** showing (a) the labeling scheme and arrangement of Cu atoms in the one-dimensional rod, (b) three-dimensional structure looking along the *a* axis. Color codes: Cu (cyan), O (red), N (blue), C (black). Symmetry codes for part a: A $-x+1, -y+1, -z+2$; B $x+1, y, z$; C $-x+2, -y+1, -z+2$.

72 h at 100 °C (Figure 7), highlighting the tight bonding of some coordinated water in the crystal lattice (Supporting Information Table S1). When the temperature was increased to 110 °C under vacuum, the sample became amorphous. A fresh sample of **2** immersed in MeOH for 12 h gave a PXRD pattern that resembles those obtained below 100 °C. Complex **2** was therefore activated at 100 °C for porosity measurements. Uptake of CO_2 gas was observed at 195 K (Figure 8), but no uptake of the larger N_2 even at 77 K.[30,48] A Brunauer–Emmett–Teller (BET) surface area of

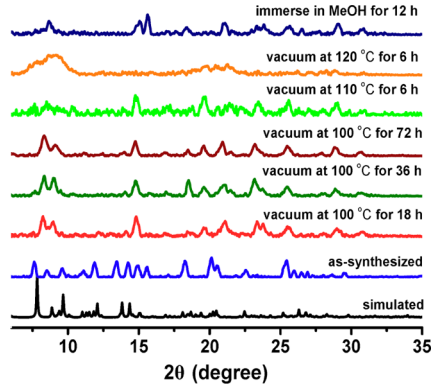

Figure 7. PXRD patterns of complex **2**.

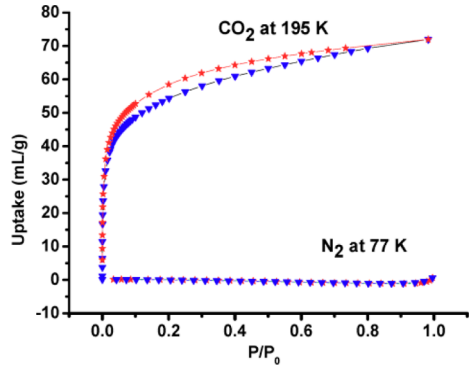

Figure 8. N_2 (77 K) and CO_2 (195 K) sorption isotherms for complex **2**. Triangular shapes indicate adsorption and five-point stars desorption. P_0 is the saturated vapor pressure of the sorbates at the measurement temperatures.

154 $m^2\ g^{-1}$ was estimated from CO_2 sorption data. Complex **2** activated at 120 °C exhibited no CO_2 or N_2 gas sorption, presumably because of the collapse of the framework structure at this temperature, as observed by PXRD. Complex **2** uptakes CO_2 over N_2 due to the larger kinetic size (kinetic diameters: 3.6 for N_2 and 3.3 Å for CO_2) of the latter which resulted in much slower diffusion rate in the 1D channel, and thereby no adsorption at low temperature of 77 K.[30] The following structural factors may also contribute to the improved CO_2 adsorption capacity of **2**: (i) the polar pyridinium–carboxylate ligand backbone,[49−51] (ii) the electrostatic interaction between C(CO_2) and O(carbonyl) from the uncoordinated carboxylate,[52] and (iii) coordinatively unsaturated metal sites in the activated sample.[53−57]

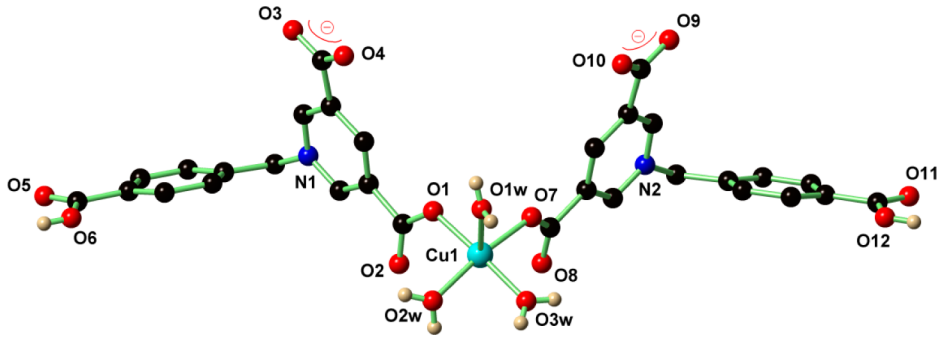

Figure 6. Structure of complex **5** with labeling scheme.

dx.doi.org/10.1021/ic500789w | *Inorg. Chem.* 2014, 53, 7446−7454

CONCLUSION

Transmetalation of $\{Na_3[Na_9(Cbdcp)_6(H_2O)_{18}]\}_n$ (**1**) with $Cu(NO_3)_2{\cdot}3H_2O$ provides easy isolation of water stable MOFs, coordination polymers, and mononuclear complexes from relatively small variations in reaction conditions. This wide variety of structures is due to the influence of the positively charged pyridinium containing ligand coupled with the flexibility imparted by the benzyl methylene. The elaborate hydrogen bonding networks in the solid state contributes to the remarkable stability, including in water. We are currently investigating potential biological applications of these charged networks that make use of this durability.[58−60]

ASSOCIATED CONTENT

Supporting Information

Selected bond distances and angles for **1**−**5**, TGA curves, PXRD pattern, and crystallographic data in CIF format. This material is available free of charge via the Internet at http://pubs.acs.org.

AUTHOR INFORMATION

Corresponding Authors

*E-mail: jxchen@smu.edu.cn.
*E-mail: zhangw@imre.a-star.edu.sg.
*E-mail: andyhor@nus.edu.sg.
*E-mail: david-young@imre.a-star.edu.sg.

Present Address

⊥Wen-Hua Zhang, College of Chemistry, Chemical Engineering and Materials Science, Soochow University, Suzhou 215123, China. Email: whzhang@suda.edu.cn

Notes

The authors declare no competing financial interest.

ACKNOWLEDGMENTS

We are grateful to the financial support from the National Natural Science Foundation of China (No. 21102070), the Program for Pearl River New Stars of Science and Technology in Guangzhou (No. 2011J2200071) and IMRE assured funding (13-1C0203).

REFERENCES

(1) Lennox, A. J. J.; Lloyd-Jones, G. C. *Angew. Chem., Int. Ed.* **2013**, *52*, 7362−7370.
(2) Gomez-Gallego, M.; Mancheno, M. J.; Sierra, M. A. *Acc. Chem. Res.* **2005**, *38*, 44−53.
(3) Roth, K. E.; Blum, S. A. *Organometallics* **2011**, *30*, 4811−4813.
(4) Peitz, S.; Peulecke, N.; Aluri, B. R.; Müller, B. H.; Spannenberg, A.; Rosenthal, U.; Al-Hazmi, M. H.; Mosa, F. M.; Wöhl, A.; Müller, W. *Organometallics* **2010**, *29*, 5263−5268.
(5) Asada, Y.; Yasuda, S.; Yorimitsu, H.; Oshima, K. *Organometallics* **2008**, *27*, 6050−6052.
(6) He, C.; Ke, J.; Xu, H.; Lei, A. *Angew. Chem., Int. Ed.* **2013**, *52*, 1527−1530.
(7) Hirner, J. J.; Shi, Y.; Blum, S. A. *Acc. Chem. Res.* **2011**, *44*, 603−613.
(8) Song, X.; Wang, Z.; Zhao, J.; Hor, T. S. A. *Chem. Commun.* **2013**, *49*, 4992−4994.
(9) Lu, Z.; Cramer, S. A.; Jenkins, D. M. *Chem. Sci.* **2012**, *3*, 3081−3087.
(10) Wang, H. M. J.; Lin, I. J. B. *Organometallics* **1998**, *17*, 972−975.
(11) Cure, J.; Poteau, R.; Gerber, I. C.; Gornitzka, H.; Hemmert, C. *Organometallics* **2012**, *31*, 619−626.
(12) Li, F.; Bai, S.; Hor, T. S. A. *Organometallics* **2008**, *27*, 672−677.
(13) Li, F.; Hu, J. J.; Koh, L. L.; Hor, T. S. A. *Dalton Trans.* **2010**, *39*, 5231−5241.
(14) Lalonde, M.; Bury, W.; Karagiaridi, O.; Brown, Z.; Hupp, J. T.; Farha, O. K. *J. Mater. Chem.* **2013**, *1*, 5453−5468.
(15) Cohen, S. M. *Chem. Rev.* **2011**, *112*, 970−1000.
(16) Tanabe, K. K.; Cohen, S. M. *Chem. Soc. Rev.* **2011**, *40*, 498−519.
(17) Sun, F.; Yin, Z.; Wang, Q.-Q.; Sun, D.; Zeng, M.-H.; Kurmoo, M. *Angew. Chem., Int. Ed.* **2013**, *52*, 4538−4543.
(18) Schneider, M. W.; Oppel, I. M.; Griffin, A.; Mastalerz, M. *Angew. Chem., Int. Ed.* **2013**, *52*, 3611−3615.
(19) Horike, S.; Kamitsubo, Y.; Inukai, M.; Fukushima, T.; Umeyama, D.; Itakura, T.; Kitagawa, S. *J. Am. Chem. Soc.* **2013**, *135*, 4612−4615.
(20) Canivet, J.; Aguado, S.; Schuurman, Y.; Farrusseng, D. *J. Am. Chem. Soc.* **2013**, *135*, 4195−4198.
(21) Zhu, W.; He, C.; Wu, P.; Wu, X.; Duan, C. *Dalton Trans.* **2012**, *41*, 3072−3077.
(22) Servalli, M.; Ranocchiari, M.; Van Bokhoven, J. A. *Chem. Commun.* **2012**, *48*, 1904−1906.
(23) Morris, W.; Doonan, C. J.; Furukawa, H.; Banerjee, R.; Yaghi, O. M. *J. Am. Chem. Soc.* **2008**, *130*, 12626−12627.
(24) Liu, D.; Lang, J.-P.; Abrahams, B. F. *J. Am. Chem. Soc.* **2011**, *133*, 11042−11045.
(25) Liu, D.; Ren, Z.-G.; Li, H.-X.; Lang, J.-P.; Li, N.-Y.; Abrahams, B. F. *Angew. Chem., Int. Ed.* **2010**, *49*, 4767−4770.
(26) Zhang, Z.; Zhang, L.; Wojtas, L.; Nugent, P.; Eddaoudi, M.; Zaworotko, M. J. *J. Am. Chem. Soc.* **2011**, *134*, 924−927.
(27) Sumida, K.; Rogow, D. L.; Mason, J. A.; McDonald, T. M.; Bloch, E. D.; Herm, Z. R.; Bae, T.-H.; Long, J. R. *Chem. Rev.* **2011**, *112*, 724−781.
(28) Higuchi, M.; Tanaka, D.; Horike, S.; Sakamoto, H.; Nakamura, K.; Takashima, Y.; Hijikata, Y.; Yanai, N.; Kim, J.; Kato, K.; Kubota, Y.; Takata, M.; Kitagawa, S. *J. Am. Chem. Soc.* **2009**, *131*, 10336−10337.
(29) Higuchi, M.; Nakamura, K.; Horike, S.; Hijikata, Y.; Yanai, N.; Fukushima, T.; Kim, J.; Kato, K.; Takata, M.; Watanabe, D.; Oshima, S.; Kitagawa, S. *Angew. Chem., Int. Ed.* **2012**, *51*, 8369−8372.
(30) Kanoo, P.; Matsuda, R.; Sato, H.; Li, L.; Jeon, H. J.; Kitagawa, S. *Inorg. Chem.* **2013**, *52*, 10735−10737.
(31) Jin, X.-H.; Sun, J.-K.; Cai, L.-X.; Zhang, J. *Chem. Commun.* **2011**, *47*, 2667−2669.
(32) Yao, Q.-X.; Pan, L.; Jin, X.-H.; Li, J.; Ju, Z.-F.; Zhang, J. *Chem.—Eur. J.* **2009**, *15*, 11890−11897.
(33) Zhang, X.-M.; Wang, Y.-Q.; Wang, K.; Gao, E.-Q.; Liu, C.-M. *Chem. Commun.* **2011**, *47*, 1815−1817.
(34) Zhu, Y.-Y.; Cui, C.; Zhang, Y.-Q.; Jia, J.-H.; Guo, X.; Gao, C.; Qian, K.; Jiang, S.-D.; Wang, B.-W.; Wang, Z.-M.; Gao, S. *Chem. Sci.* **2013**, *4*, 1802−1806.
(35) Sheldrick, G. M. *SADABS. Program for Empirical Absorption Correction of Area Detector Data*; University of Göttingen: Göttingen, Germany, 1996.
(36) Sheldrick, G. M. *SHELXS-97 and SHELXL-97. Programs for Crystal Structure Solution and Refinement*; University of Göttingen: Göttingen, Germany, 1997.
(37) Farrugia, L. *J. Appl. Crystallogr.* **1999**, *32*, 837−838.
(38) Spek, A. *J. Appl. Crystallogr.* **2003**, *36*, 7−13.
(39) Ruben, M.; Rojo, J.; Romero-Salguero, F. J.; Uppadine, L. H.; Lehn, J.-M. *Angew. Chem., Int. Ed.* **2004**, *43*, 3644−3662.
(40) Matthew, E. C.; Mary, S. C.; Darren, W. J. *Chem. Soc. Rev.* **2014**, *43*, 1825−1834.
(41) Li, H.; Eddaoudi, M.; O'Keeffe, M.; Yaghi, O. M. *Nature* **1999**, *402*, 276−279.
(42) Brozek, C. K.; Dincă, M. *J. Am. Chem. Soc.* **2013**, *135*, 12886−12891.
(43) Deng, H.; Doonan, C. J.; Furukawa, H.; Ferreira, R. B.; Towne, J.; Knobler, C. B.; Wang, B.; Yaghi, O. M. *Science* **2010**, *327*, 846−850.
(44) Yaghi, O. M.; O'Keeffe, M.; Ockwig, N. W.; Chae, H. K.; Eddaoudi, M.; Kim, J. *Nature* **2003**, *423*, 705−714.
(45) Eddaoudi, M.; Kim, J.; Rosi, N.; Vodak, D.; Wachter, J.; O'Keeffe, M.; Yaghi, O. M. *Science* **2002**, *295*, 469−472.
(46) Kumar, G.; Gupta, R. *Inorg. Chem.* **2012**, *51*, 5497−5499.
(47) Zhang, Z.; Wojtas, L.; Eddaoudi, M.; Zaworotko, M. J. *J. Am. Chem. Soc.* **2013**, *135*, 5982−5985.

(48) Dybtsev, D. N.; Chun, H.; Yoon, S. H.; Kim, D.; Kim, K. *J. Am. Chem. Soc.* **2004**, *126*, 32−33.
(49) Demessence, A.; D'Alessandro, D. M.; Foo, M. L.; Long, J. R. *J. Am. Chem. Soc.* **2009**, *131*, 8784−8786.
(50) Torrisi, A.; Bellandm, R. G.; Mellot-Draznieks, C. *Cryst. Growth Des.* **2010**, *10*, 2839−2841.
(51) Mu, W.; Liu, D.; Yang, Q.; Zhong, C. *Microporous Mesoporous Mater.* **2010**, *130*, 76−82.
(52) Torrisi, A.; Mellot-Draznieks, C.; Bell, R. G. *J. Chem. Phys.* **2010**, *132*, 044705.
(53) McDonald, T. M.; D'Alessandro, D. M.; Krishna, R.; Long, J. R. *Chem. Sci.* **2011**, *2*, 2022−2028.
(54) Dincâ, M.; Han, W. S.; Liu, Y.; Dailly, A.; Brown, C. M.; Long, J. R. *Angew. Chem., Int. Ed.* **2007**, *46*, 1419−1422.
(55) Ma, F.-J.; Liu, S.-X.; Sun, C.-Y.; Liang, D.-D.; Ren, G.-J.; Wei, F.; Chen, Y.-G.; Su, Z.-M. *J. Am. Chem. Soc.* **2011**, *133*, 4178−4181.
(56) Gong, Y.-N.; Meng, M.; Zhong, D.-C.; Huang, Y.-L.; Jiang, L.; Lu, T.-B. *Chem. Commun.* **2012**, *48*, 12002−12004.
(57) Ma, S.; Zhou, H.-C. *J. Am. Chem. Soc.* **2006**, *128*, 11734−11735.
(58) Chen, J.-X.; Lin, W.-E.; Chen, M.; Que, F.-C.; Tao, L.; Cen, X.-L.; Zhou, Y.-M.; Chen, W.-H. *Inorg. Chim. Acta* **2014**, *409* (Part B), 195−201.
(59) Chen, M.; Chen, M.-Z.; Zhou, C.-Q.; Lin, W.-E.; Chen, J.-X.; Chen, W.-H.; Jiang, Z.-H. *Inorg. Chim. Acta* **2013**, *405*, 461−469.
(60) Chen, J.-X.; Lin, W.-E.; Zhou, C.-Q.; Yau, L. F.; Wang, J.-R.; Wang, B.; Chen, W.-H.; Jiang, Z.-H. *Inorg. Chim. Acta* **2011**, *376*, 389−395.